The Elastic-Plastic Micromechanical Response of the Particle Volume Fraction and the Average Size of Particles

YONG-MING GUO
Integrated Arts and Sciences Area
Kagoshima University
1-21-30 Korimoto, Kagoshima City, 890-0065
JAPAN
guoy@km.kagoshima-u.ac.jp http://ris.kuas.kagoshima-u.ac.jp/html/100005102_en.html

KENTO MORIKI
Department of Mechanical Engineering
Kagoshima University
1-21-40 Korimoto, Kagoshima City, 890-0065
JAPAN
k4613050@kadai.jp

Abstract: - In microstructural parameters, the particle volume fraction and the average size of particles are important factors which determine the mechanical properties of materials. While, studies of three-dimensional microstructure-property relationships are still less. In this research, for two-phase materials, we have calculated elastic-plastic micromechanical responses of the particle volume fraction and the average size of particles using a commercial software package, as a basic study of three-dimensional microstructure-property relationships, in which the 3-D FEM is used. Although the grain sizes and the grain shapes of the actual materials are non-uniform, we use a simple virtual material model with particles of uniform size and shape to investigate the influence of the average size of the particles. In order to investigate the elastic-plastic micromechanical response of the particle volume fraction, two kinds of the particle volume fraction are used. By analyzing the calculated results of Von Mises stress, the equivalent plastic strain, and the curve of average tensile stress – tensile rate, some new knowledges on three-dimensional microstructure-property relationships have obtained. The advantage of using the 3-D FEM is that it is possible to study the three-dimensional microstructure-property relationships by easily and inexpensively changing various microstructural parameters (not only the particle volume fraction and the average size of particles).

Key-Words: - FEM, Microstructure-property relationships, Microstructural parameters, Particle volume fraction, Average size of particles, Elastic-plasticity

1 Introduction

It is well known that the properties of materials are a function of their microstructural parameters such as the particle volume fraction, the contiguity of particles, and the average size of particles, etc. The microstructural parameters are obtained from materials characterization that is usually based on data obtained from two-dimensional plane sections for most crystalline materials. However, many effects of the microstructural units on the properties of materials are three-dimensional, because most materials have a polycrystalline or multi-phase structure with significant complexity in the spatial arrangement of their microstructural units. Therefore, it is necessary to use the microstructural parameters indicated by three-dimensional microstructural units and to estimate three-dimensional microstructural features of materials directly. The serial-sectioning methods [1, 2, 3] can be used for this purpose. While this approach is hard to be implemented, for example, it gives actual data on various microstructural parameters, but in order to use them as inputs for property studies of materials with three-dimensional microstructural units, one must re-construct many samples of materials. The numerical method is a good selection for studies of three-dimensional microstructure-property relationships. The fast Fourier transform-based method has been used in numerical modelling of three-dimensional microstructure-property relationships [4, 5, 6]. But, the fast Fourier transform-based method has some demerits, such as the lack of a conformal representation of grain boundaries. The crystal-plasticity finite-element

method (CP-FEM) has been shown to be capable of describing metal forming problems, (for example, [7, 8]). While, to perform a CP-FEM analysis, many material parameters have to be empirically determined, so that deviations of these parameters may cause errors in the CP-FEM analysis.

The finite element method (FEM) is a powerful method in numerical methods especially for simulations of three-dimensional problems (for example, [9, 10]). One can conveniently make various kinds of elements using commercial software packages to capture the real microstructural complexities of materials. The elements of micro-scale and three-dimension have to be used in order to indicate microstructural units, and a large number of elements are necessary. Therefore, the pre-processing for the numerical calculation is very troublesome. It is a challenge, but it can be achieved when using commercial software packages of the FEM. In fact, such a challenge exists in all the numerical methods. That there are commercial software packages of the FEM instead of other numerical methods is a key which can meet such a challenge. While, studies of three-dimensional microstructure-property relationships using the FEM are still less. In microstructural parameters, the particle volume fraction (PVF) and the average size of particles are important factors which determine the mechanical properties of materials. In this research, we would calculate elastic-plastic micromechanical responses of the particle volume fraction and the average size of particles for two-phase materials using a commercial software package called MARC Mentat, as a basic study of three-dimensional microstructure-property relationships, in which the 3-D FEM is used.

2 The Object and Method of Calculation

In the actual materials, the particle distribution is typically random. For the micromechanical modeling of the materials, one may choose a representative volume element (RVE) to describe the microstructural features of materials and then to numerically obtain the overall mechanical behaviors of the materials. In this work, as the RVE for modelling, a cube of $1\times1\times1$ is calculated, and the domain coordinates of the cube are taken as (0, 0, 0) $\times$(1, 1, 1). Although the unit of the cube's size is not given, a unit with grain level is considered and used in this work. The tensile boundary condition, that z direction's displacements of nodes located at surface of z=1 are +0.2 (20% tensile rate), is imposed. The constraint boundary conditions, that x direction's displacements of nodes located at surface of x=0 are 0, that y direction's displacements of nodes located at surface of y=0 are 0, and that z direction's displacements of nodes located at surface of z=0 are 0, are also imposed.

It is well known that the average grain size of the crystalline material generally plays a very significant role. Thus, the strength of all polycrystalline materials is related to the grain size, d, through the Hall–Petch equation which states that the yield stress, σ_y is given by

$$\sigma_y = \sigma_0 + k_y d^{-\frac{1}{2}} \tag{1}$$

where σ_0 is termed the friction stress and k_y is a constant of yielding [11, 12]. Although the grain sizes and the grain shapes of the actual materials are

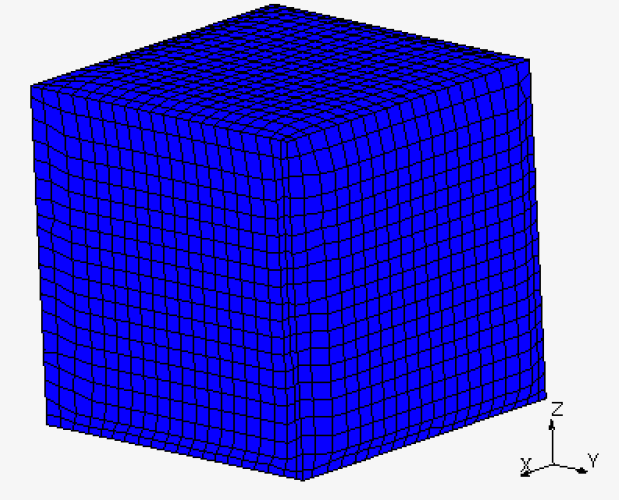

Fig. 1. The model of 8000 elements.

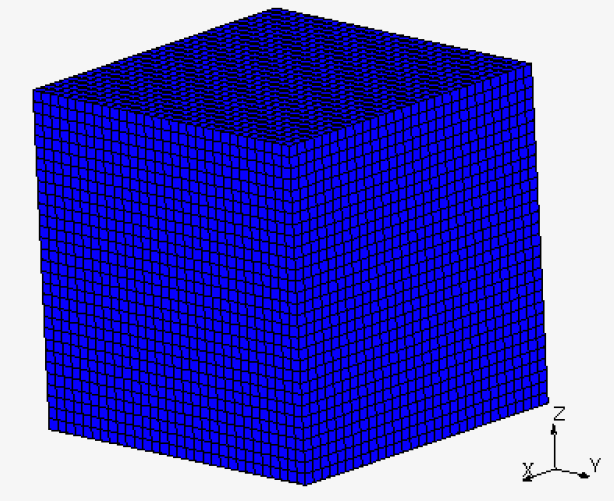

Fig. 2. The model of 27000 elements.

non-uniform, in this paper we use a simple virtual material model with particles of uniform size and shape to investigate the influence of the average size of the particles. In order to investigate the elastic-plastic micromechanical response of the average size of particles, two FE models are used, in which the cube is divided into 8000 (average volume of particles is 1/8000) (Fig. 1) and 27000 (average volume of particles is 1/27000) (Fig. 2) hexahedral elements, respectively.

In order to investigate the elastic-plastic micromechanical response of the PVF of two-phase materials, in this study two kinds of the PVF of hard phase, which are 10% and 20%, respectively, are used, for the two FE models. The locations of elements of hard phase are randomly selected in inside and at the surface of the cube. For example, the distribution of PVF 20% of hard phase for 27000 elements model is shown in Fig. 3.

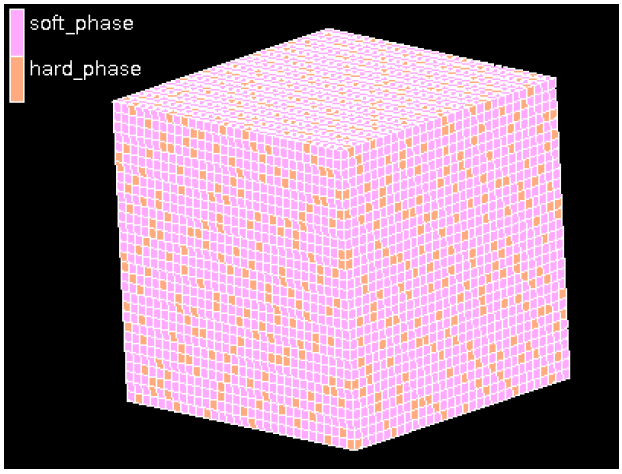

(a) Outside view

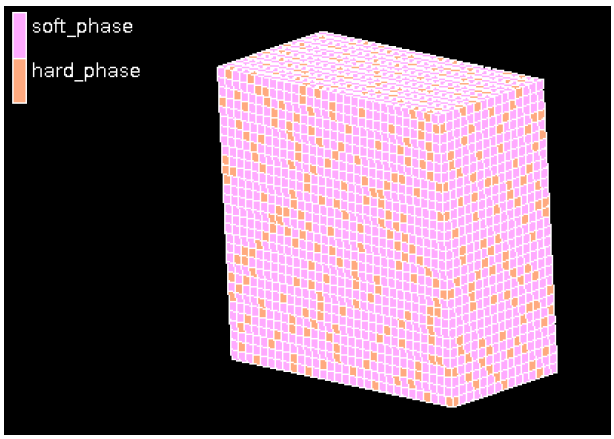

(b) Sectional view

Fig. 3. The distribution of PVF 20% of hard phase for 27000 elements model.

The Young's modulus E and Poisson's ratio ν for the elastic FE calculation are shown in Table 1, and the flow-stress equations for the plastic FE calculation are shown in Table 2, where $\bar{\sigma}$ is Von Mises equivalent stress and $\bar{\varepsilon}$ is the equivalent strain.

Table 1. The Young's modulus E and Poisson's ratio ν for the elastic FE calculation

Soft_phase	E=80 GPa	ν=0.3
Hard_phase	E=150 GPa	ν=0.3

Table 2. The flow-stress equations for the plastic FE calculation

Soft_phase	$\bar{\sigma}=240\times \bar{\varepsilon}^{0.03}$ MPa
Hard_phase	$\bar{\sigma}=900\times \bar{\varepsilon}^{0.09}$ MPa

3 The Results of Calculation

3.1 The Von Mises Stress

For the case of the PVF 10% of hard phase using 8000 elements, the distribution of Von Mises stresses at 0.4% tensile rate is shown as Fig. 4, and the distribution of Von Mises stresses at 20% tensile rate is shown as Fig. 5. As expected, it can be seen from these figures that the maximum value and average value of Von Mises stresses at 20% tensile rate are larger than those values at 0.4% tensile rate, respectively.

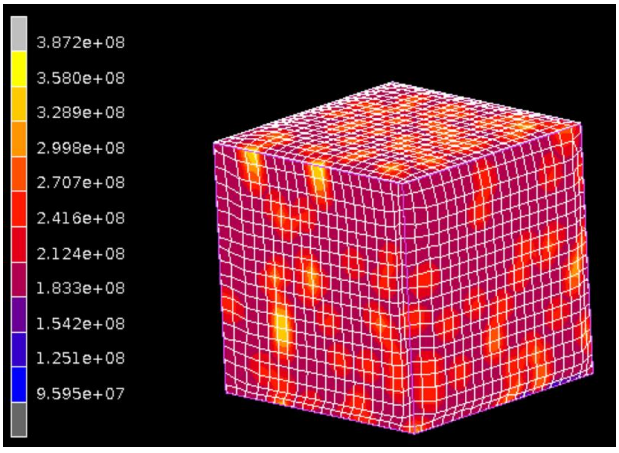

Fig. 4. Von Mises stresses (Pa) of the PVF 10% for 0.4% tensile rate using 8000 elements.

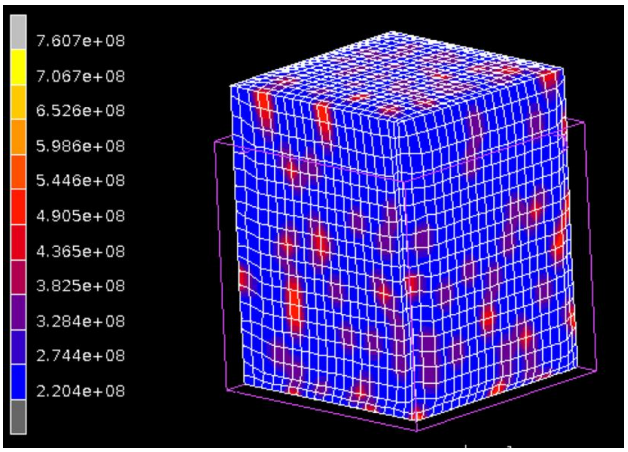

Fig. 5. Von Mises stresses (Pa) of the PVF 10% for 20% tensile rate using 8000 elements.

For the case of the PVF 20% of hard phase using 8000 elements, the distribution of Von Mises stresses at 0.4% tensile rate (using 8000 elements) is shown as Fig. 6, and the distribution of Von Mises stresses at 20% tensile rate (using 8000 elements) is shown as Fig. 7. As expected, it can be seen from these figures, that for the model of PVF 20% of hard phase, the maximum (or average) value of Von Mises stress at 20% tensile rate is larger than the value at 0.4% tensile rate. In addition, many oblique large stress bands are clearly seen form the both figures.

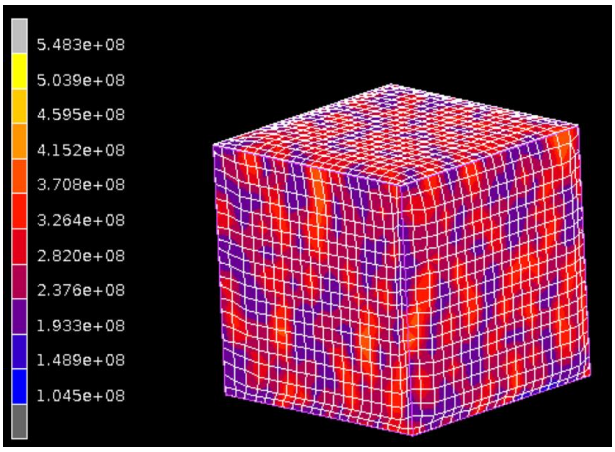

Fig. 6. Von Mises stresses (Pa) of the PVF 20% for 0.4% tensile rate using 8000 elements.

For the case of the PVF 10% of hard phase using 27000 elements, the distribution of Von Mises stresses at 0.4% tensile rate is shown as Fig. 8, and the distribution of Von Mises stresses at 20% tensile rate is shown as Fig. 9. It is similar to that of the 8000 element model, it can be seen from these figures, for the model of PVF 10% of hard phase using 27000 elements, that at 20% tensile rate, the

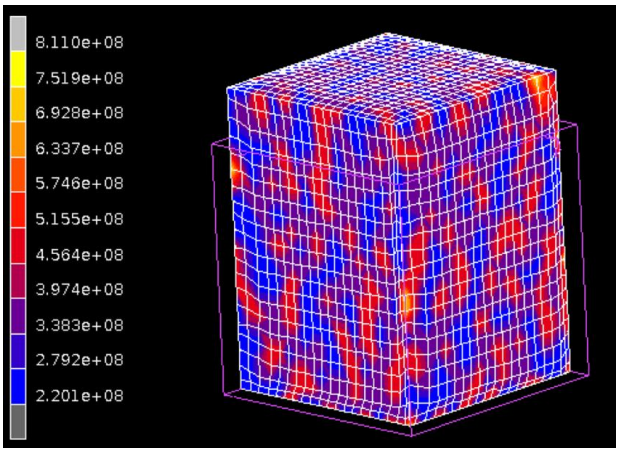

Fig. 7. Von Mises stresses (Pa) of the PVF 20% for 20% tensile rate using 8000 elements.

maximum (or average) value of Von Mises stress is larger than the value at 0.4% tensile rate. In addition, many oblique large stress bands are clearly seen

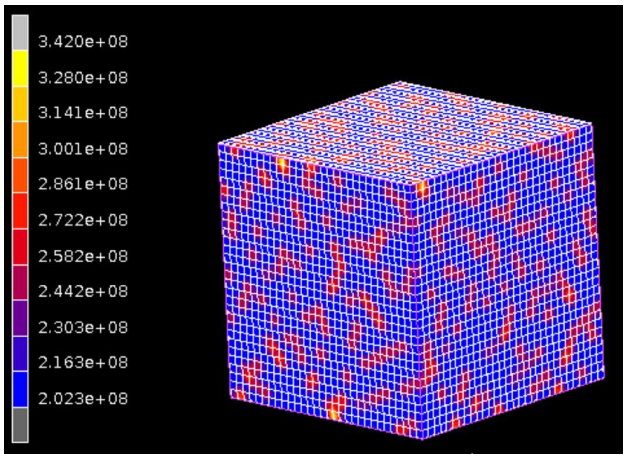

Fig. 8. Von Mises stresses (Pa) of the PVF 10% for 0.4% tensile rate using 27000 elements.

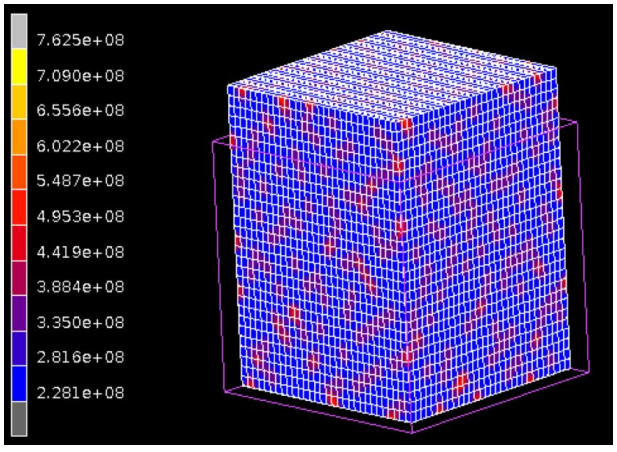

Fig. 9. Von Mises stresses (Pa) of the PVF 10% for 20% tensile rate using 27000 elements.

from the both figures for the model of PVF 10% of hard phase, too. Moreover, it can be seen from Fig. 4, Fig. 5, Fig. 8, and Fig. 9, that for the PVF 10% of hard phase, the distribution and magnitudes of Von Mises stresses using 27000 elements are difference from those using 8000 elements.

For the case of the PVF 20% of hard phase using 27000 elements, the distribution of Von Mises stresses at 0.4% tensile rate is shown as Fig. 10, and the distribution of Von Mises stresses at 20% tensile rate is shown as Fig. 11. It can be also seen from these figures, it is similar to the case using 8000 element model, that, for the model of PVF 20% of hard phase, the maximum (or average) value of Von Mises stresses at 20% tensile rate is larger than the value at 0.4% tensile rate. Many oblique large stress bands are clearly seen. Moreover, it can be seen from Fig. 6, Fig. 7, Fig. 10, and Fig. 11, that, for the PVF 20% of hard phase, the distribution and magnitudes of Von Mises stresses using 27000 elements are difference from those using 8000 elements.

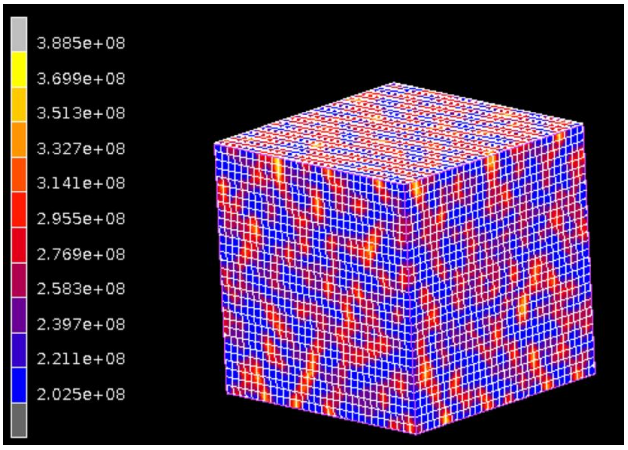

Fig. 10. Von Mises stresses (Pa) of the PVF 20% for 0.4% tensile rate using 27000 elements.

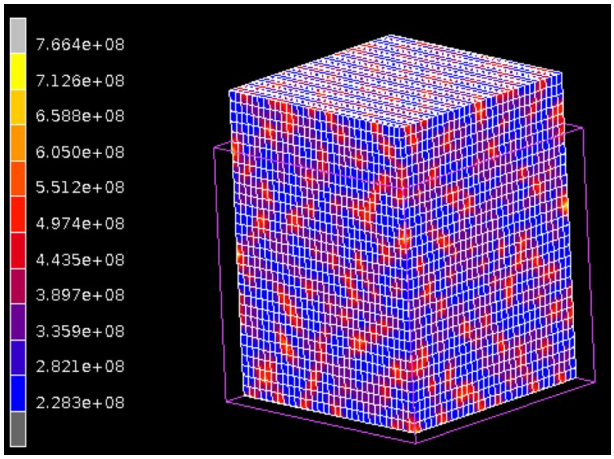

Fig. 11. Von Mises stresses (Pa) of the PVF 20% for 20% tensile rate using 27000 elements.

3.2 The Equivalent Plastic Strain

For the case at 1% tensile rate using 8000 elements, the distribution of equivalent plastic strains of the PVF 10% of hard phase is shown as Fig. 12, and the distribution of equivalent plastic strains of the PVF 20% of hard phase is shown as Fig. 13. It can be seen from these figures, that the maximum (or average) value of equivalent plastic strains of the PVF 20% of hard phase is larger than the value of the PVF 10% of hard phase. In addition, as expected, many oblique large equivalent plastic strains bands are clearly seen form the both figures.

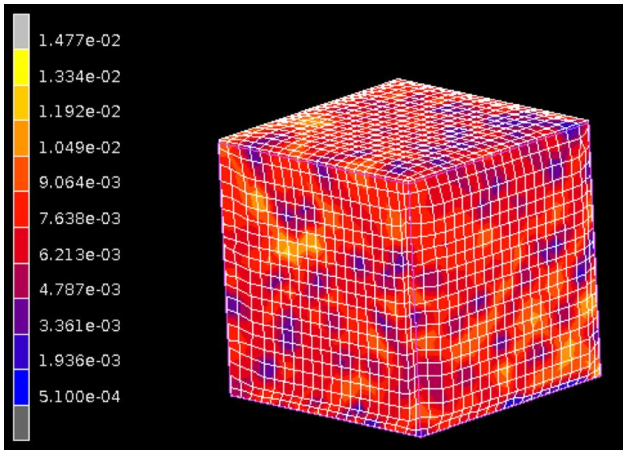

Fig. 12. Equivalent plastic strains of the PVF 10% for 1% tensile rate using 8000 elements.

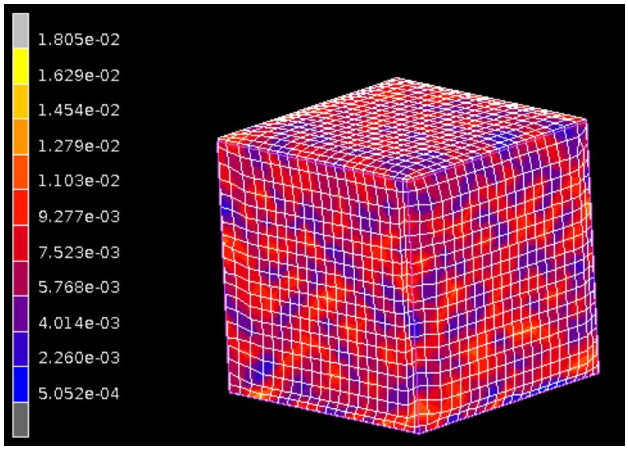

Fig. 13. Equivalent plastic strains of the PVF 20% for 1% tensile rate using 8000 elements.

For the case at 1% tensile rate using 27000 elements, the distribution of equivalent plastic strains of the PVF 10% of hard phase is shown as Fig. 14, the distribution of equivalent plastic strains

of the PVF 20% of hard phase is shown as Fig. 15. It can be seen from these figures that the maximum (or average) value of equivalent plastic strains of the PVF 20% of hard phase is larger than the value of the PVF 10% of hard phase. In addition, as expected, many oblique large equivalent plastic strains bands are clearly seen form the both figures. Moreover, it can be seen from Fig. 12, Fig. 13, Fig. 14, and Fig. 15, that the distribution and magnitudes of equivalent plastic strains using 27000 elements are difference from those using 8000 elements, at 1% tensile rate.

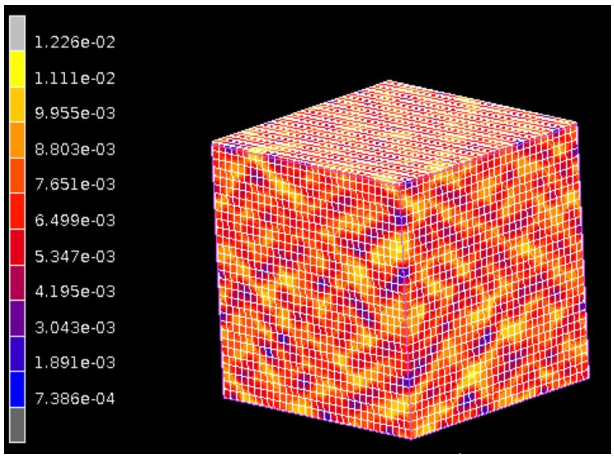

Fig. 14. Equivalent plastic strains of the PVF 10% for 1% tensile rate using 27000 elements.

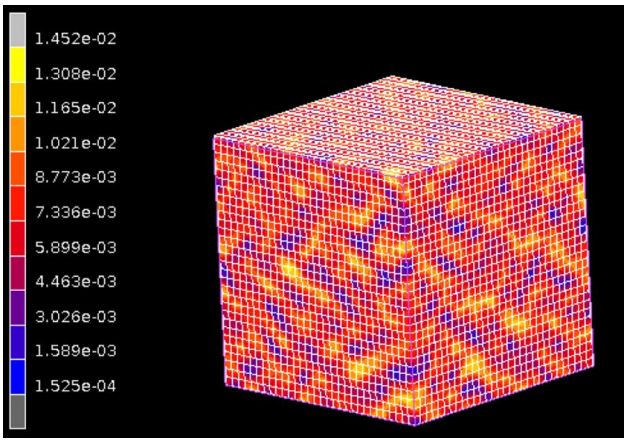

Fig. 15. Equivalent plastic strains of the PVF 20% for 1% tensile rate using 27000 elements.

For the case at 20% tensile rate using 27000 elements, the distribution of equivalent plastic strains of the PVF 10% of hard phase is shown as Fig. 16, and the distribution of equivalent plastic strains of the PVF 20% of hard phase is shown as Fig. 17. It can be seen from these figures that the maximum value of equivalent plastic strains of the PVF 20% of hard phase is larger than that of the PVF 10% of hard phase. In addition, as expected, many oblique large equivalent plastic strains bands are clearly seen form the both figures, too.

3.3 The Curve of Average Tensile Stress – Tensile Rate

The curves of *z* direction's average tensile stress – tensile rate of the cube using 8000 elements are shown as Fig. 18, and the curves of *z* direction's average tensile stress – tensile rate of the cube using 27000 elements are shown as Fig. 19, where *s* is the *z* direction's average tensile stress and *e* is the tensile rate. As expected, it can be seen from these figures that the *z* direction's average tensile stresses of the cube increase along with the increase of the PVF for both element models. In addition, it can be seen from these figures that the work hardening increases along with the increase of the PVF for

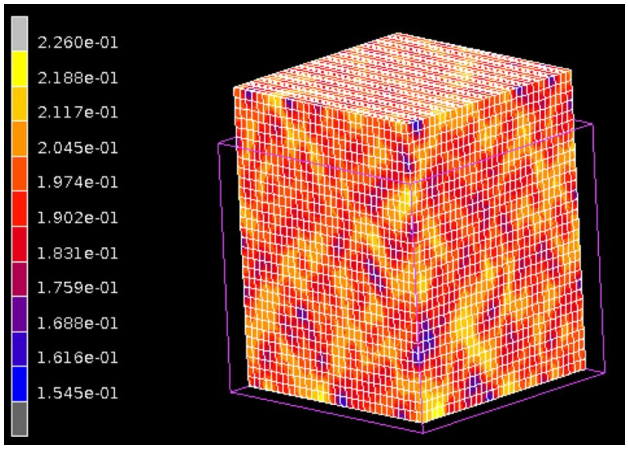

(a) Outside view

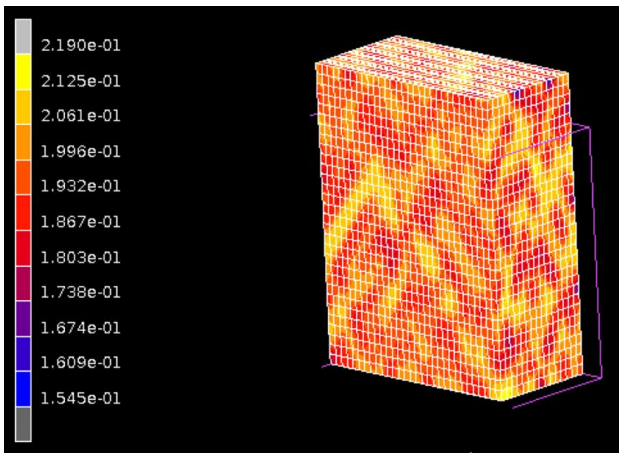

(b) Sectional view

Fig. 16. Equivalent plastic strains of the PVF 10% for 20% tensile rate using 27000 elements.

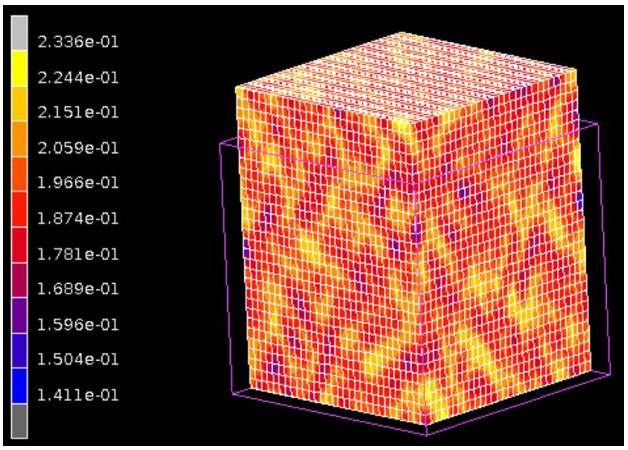

(a) Outside view

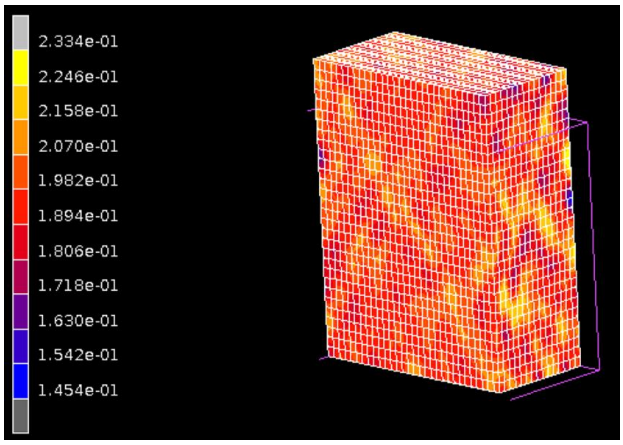

(b) Sectional view

Fig. 17. Equivalent plastic strains of the PVF 20% for 20% tensile rate using 27000 elements.

both element models. Moreover, it can be seen from Fig. 18 and Fig. 19, that the values of *z* direction's average tensile stress of both PVFs using 27000 elements are larger than those of both PVFs using 8000 elements, respectively.

4 Conclusion

In this research, we have calculated elastic-plastic micromechanical response of the particle volume fraction and the average size of particles of two-phase materials using a commercial software package. It may be said that the commercial software package of the FEM is an effective and powerful tool for calculating elastic-plastic micromechanical response of the particle volume fraction and the average size of particles, and some new knowledges on three-dimensional microstructure-property relationships have obtained by simulating using the 3-D FEM. The direction for

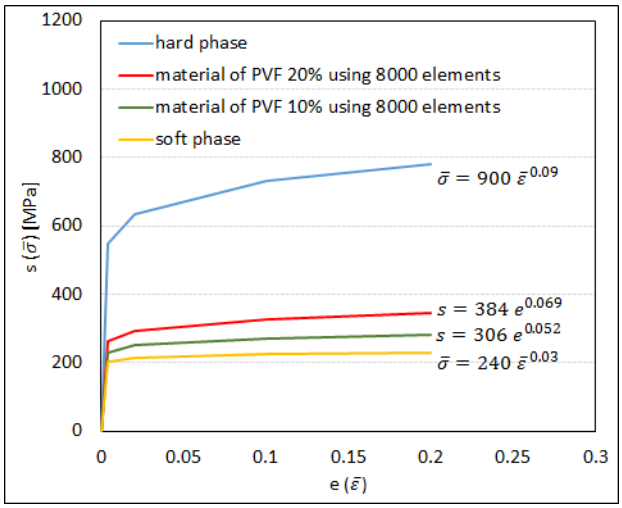

Fig. 18. The curves of s – e using 8000 elements.

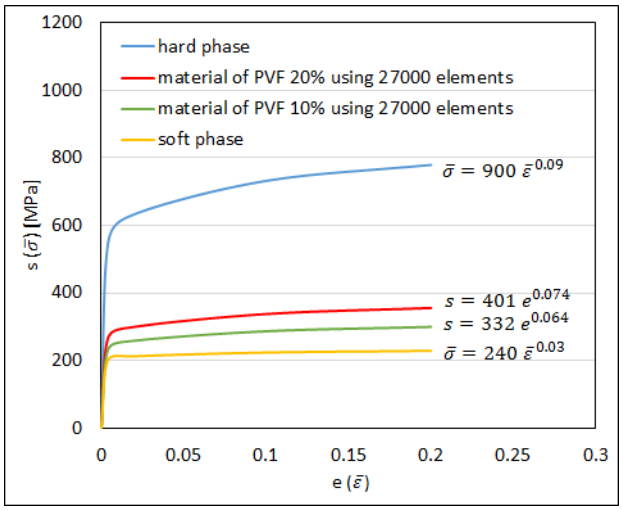

Fig. 19. The curves of s – e using 27000 elements.

future research is investigating the influence of particles with non-uniform size and shape which are near to the actual materials.

References:

[1] A. Tewari, A.M. Gokhale, Estimation of Three Dimensional Grain Size Distribution from Microstructural Serial Sections, *Materials Characterization*, Vol. 46, 2001, pp. 329-335.

[2] D.M. Saylor, A. Morawiec and G.S. Rohrer, Distribution and Energies of Grain Boundaries in Magnesia as a Function of Five Degrees of Freedom, *Journal of the American Ceramic Society*, Vol. 85, 2002, pp. 3081-3083.

[3] D.J. Rowenhurst, A. Gupta, C.R. Feng and G. Spanos, 3D Crystallographic and Morphological Analysis of Coarse Martensite: Combining EBSD

and Serial Sectioning, *Scripta Materialia*, Vol. 55, 2006, pp. 11-16.
[4] H. Moulinec, P. Suquet, A Numerical Method for Computing the Overall Response of Nonlinear Composites with Complex Microstructure, *Computer Methods in Applied Mechanics and Engineering*, Vol. 157, 1998, pp. 69-94.
[5] J.C. Michel, H. Moulinec and P. Suquet, A Computational Method Based on Augmented Lagrangians and Fast Fourier Transforms for Composites with High Contrast, *Computer Modeling in Engineering and Sciences*, Vol. 1, 2000, pp. 79-88.
[6] R.A. Lebensohn, M. Motagnat, P. Mansuy, P. Duval, J. Meysonnier and A. Philip, Modeling Viscoplastic Behavior and Heterogeneous Intracrystalline Deformation of Columnar Ice Polycrystals, *Acta Materialia*, Vol. 57, 2009, pp. 1405-1415.
[7] A.J. Beaudoin, P.R. Dawson, K.K. Mathur, U.F. Kocks and D.A. Korzekwa, Application of Polycrystal Plasticity to Sheet Forming, *Computer Methods in Applied Mechanics and Engineering*, Vol. 117, 1994, pp. 49-70.
[8] S. Yuan, M. Huang, Y. Zhu, and Z. Li, A Dislocation Climb/glide Coupled Crystal Plasticity Constitutive Model and Its Finite Element Implementation, *Mechanics of Materiais*, Vol. 118, 2018, pp. 44-61.
[9] N. Chawal, V.V. Ganesh and B. Wunsch, Three-Dimensional (3D) Microstructure Visualization and Finite Element Modeling of the Mechanical Behavior of SiC Particle Reinforced Aluminum Composites, *Scripta Materialia*, Vol. 51, 2004, pp. 161-165.
[10] N. Chawal, R.S. Sidhu and V.V. Ganesh, Three-Dimensional Visualization and Microstructure-Based Modeling of Deformation in Particle-Reinforced Composites, *Acta Materialia*, Vol. 54, 2006, pp. 1541-1548.
[11] E.O. Hall, The Deformation and Ageing of Mild Steel: III Discussion of Results, *Proceedings of the Physical Society, Section B*, Vol.64, 1951, pp. 747-753.
[12] N.J. Petch, The Cleavage Strength of Polycrystals, *Journal of the Iron and Steel Institute*, Vol. 174, 1953, pp. 25-28.